Research Article | Vol. 1, No. 1 | 15 Sep 2018 | OSA CONTINUUM 56
OSA CONTINUUM

In-fiber polarizer based on a 45-degree tilted fluoride fiber Bragg grating for mid-infrared fiber laser technology

GAYATHRI BHARATHAN,* DARREN D. HUDSON, ROBERT I. WOODWARD, STUART D. JACKSON, AND ALEX FUERBACH

MQ Photonics Research Centre, Faculty of Science and Engineering, Macquarie University, New South Wales 2109, Australia
*gayathri.bharathan@students.mq.edu.au

Abstract: We report the direct femtosecond laser inscription of a 45° tilted fiber Bragg grating (TFBG) into fluoride fiber, creating an in-fiber mid-infrared polarizer. Utilizing a 16 mm long intracavity TFBG, we demonstrate a 2.862 μm $Ho^{3+}Pr^{3+}$:ZBLAN fiber laser with 21.6 dB output polarization extinction ratio (PER), up to 0.37 W output power and 31.3% slope efficiency. In addition, we experimentally demonstrate that the laser PER is a linear function of grating length. Our results show that fluoride TFBGs are a promising route to replace bulk polarizers in mid-IR laser cavities, paving the way to all-fiber mid-infrared laser systems.

1. Introduction

In-fiber polarizers based on tilted fiber Bragg grating (TFBG) technology have been extensively investigated in the near-infrared (near-IR) region for the last decade using silica fibers [1–4]. However, above 2.5 μm wavelengths the performance of silica fibers deteriorates and losses increase dramatically. Moving to longer wavelengths near 3 μm, silica glass becomes virtually opaque and thus unsuitable for the development of fiber laser sources. Also, the high phonon energy of silica prohibits mid-infrared (mid-IR) laser transitions since phonons cause strong non-radiative relaxation of excitation, rather than radiative emission. In order to achieve low phonon energies, the host lattice needs to have heavy atoms bound together with bonds that display low spring constants (i.e. weakly bound) [5]. Fluoride and chalcogenide glasses have low phonon energy, good mid-IR transparency and are chemically stable. ZBLAN (ZrF_4-BaF_2-LaF_3-AlF_3-NaF) is considered to be the most stable heavy metal fluoride glass and represents an excellent host for rare-earth ions. This glass has been extensively used for its benefits such as wide transparency window and low phonon energy (565 cm^{-1}) when compared to silica glass (1100 cm^{-1}) [5,6].

Fiber lasers based on rare earth doped ZBLAN fibers constitute high brightness diffraction-limited mid-IR sources. However, the output of these lasers is usually unpolarized due to the lack of polarization selective components in the laser cavity. On the other hand, linear polarized mid-IR fiber lasers are useful light sources which can enhance various nonlinear effects like supercontinuum generation [7] and enable new sensing approaches like polarization spectroscopy [8]. In order to achieve an alignment free polarized all-fiber mid-IR laser system, in-fiber polarizers are required. 45° TFBGs are a promising concept for developing in-fiber polarizers. The individual grating planes are tilted at Brewster's angle and therefore the device transmits *p*-polarized light with low loss but couples *s*-polarized light into radiation modes [9]. Fully fiberized mid-IR lasers have recently been developed using uniform fiber Bragg gratings (FBGs) as narrowband cavity mirrors [10–12]. However, their polarization properties have yet to be explored and linear polarized mid-IR sources currently still require bulk optical elements.

#332357 https://doi.org/10.1364/OSAC.1.000056
Journal © 2018 Received 22 May 2018; accepted 23 Jul 2018; published 12 Sep 2018

OSA CONTINUUM

The first TFBG was demonstrated by Erdogan *et al.* in 1996 [1]. Later, TFBGs were used for various applications such as in-line polarimeters [2], optical sensors [3] and non-linear polarization rotation mode-locking [4]. Recently, Zhou *et al.* fabricated a 50 mm long 45° TFBG in silica fiber with a strong polarization extinction ratio (PER) of 33 dB, which was shown to be an ideal polarizer to achieve linear polarized laser operation at 1550 nm [13]. All these results were demonstrated in the near-IR spectral region. In addition, in all these reports the TFBGs were fabricated using an ultra-violet (UV) inscription process which requires an expensive separate phase-mask for each TFBG design. Direct femtosecond laser (fs laser) inscription represents an attractive alternative [11,14,15]. This flexible fabrication technique enables complete control over period, tilt angle and length of the grating. In 2017, Ioannou *et al.* reported the plane-by-plane direct inscription of 7° TFBG in silica fiber using a fs laser [16]. In this paper, we report the fabrication of a 45° TFBG using the core-scanned method by focusing a fs laser directly into the core of passive and active ZBLAN fibers, thereby extending the concept of in-fiber polarizers to soft glass fibers for the first time. This resulted in a highly linear polarized (PER=21.6 dB) all-fiber mid-IR laser with excellent long-term stability. The slope efficiencies of the laser with and without a TFBG were analyzed, and the PER response of the laser as a function of grating length was measured.

2. Working principle of TFBG

A fiber grating consists of a periodic structure of two layer materials with slightly different refractive indices, n_1 and n_2. Typically, the refractive index modulation (Δn=n_1-n_2) is on the order of 10^{-3} to 10^{-5} [9]. The amplitude of reflection from a grating depends on the index contrast at each interface. To achieve polarization selective loss, thus forming an in-fiber polarizer, the grating planes have to be tilted by an angle θ which is determined by the Brewster angle of the interface. The ratio of the two refractive indices, $\tan\theta = (n_1/n_2)$, which is approximately equal to 1, defines the Brewster angle as 45°. Therefore, a 45° TFBG acts as a strong in-fiber polarizer which partially couples *s*-polarized light out of the fiber and transmits *p*-polarized light in the fiber as shown schematically in Fig. 1(a).

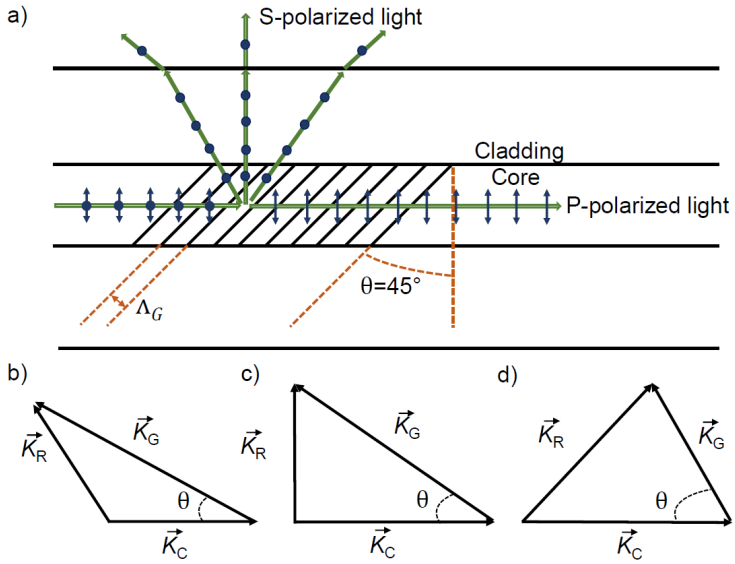

Fig. 1. (a) Schematic diagram of the TFBG in radiation coupling mode. Phase-matching conditions of TFBG with (b) small tilt angles (c) tilt angle = 45° and (d) large tilt angles.

OSA CONTINUUM

By taking total internal reflection (TIR) into consideration, the vector model of the phase-matching conditions to identify the mode coupling regimes of TFBGs at various tilt angles are illustrated in Figs. 1(b)–1(d). When a beam of light is incident on a tilted grating structure, its components are radiated out in various directions with different strengths. The strongest coupling arises at the phase-matching condition [17]

$$\vec{K_R} = \vec{K_C} + \vec{K_G}, \tag{1}$$

where $\vec{K_R}$, $\vec{K_C}$ and $\vec{K_G}$ are wave vectors of the radiated light, core mode and the grating, respectively. As shown in Fig. 1(b), for small tilt angles, the core mode is coupled into backward propagating cladding modes. Similarly, when the grating structure is tilted at very large angles, the forward propagating core modes will be coupled into forward propagating cladding modes as illustrated in Fig. 1(d). In both these cases, a series of comb like resonances can be observed in the transmission spectrum due to the backward and forward coupling to different cladding modes and this effect can be effectively utilized for sensing applications [17]. However, in the case of in-fiber polarizers, the light will be stripped out from the fiber as leaky modes. From Fig. 1(c), we can clearly see that if the tilt angle $\theta = 45°$, the phase matched light will be completely radiated out of the fiber cladding as no cladding modes can be excited in this case. On the other hand, there is also a range of tilt angles in which the light will not be confined inside the cladding of the fiber but radiated out as leaky modes from the fiber. The range of tilt angles which enables radiation mode coupling depends on the critical angle of the fiber, $\alpha_c = \arcsin(n_a/n_2)$, where n_a and n_2 are the refractive indices of the surrounding medium and cladding, respectively [17]. The calculated critical angle by considering the fact that the fiber is surrounded by air ($n_a = 1$) is $\alpha_c = 42.7°$. Thus, the tilt angle θ should be within the range of 23.7° and 66.4° to initiate radiation coupling out of the fiber. Below and beyond this range the light will be coupled into the cladding mode in the backward and forward direction and get confined inside the cladding. For a 45° TFBG, the strongest coupling wavelength can be expressed as [18]

$$\lambda_{\text{strongest}} = \frac{2n_{\text{eff}}\Lambda_G \cos 45°}{m}, \tag{2}$$

where n_{eff} is the effective index of refraction of the core, Λ_G is the normal grating period as shown in Fig.1(a) and m is the order of the grating. In our experiments, a second-order grating was chosen to avoid any overlap between closely spaced adjacent grating planes.

3. Characterization of the 45° TFBG

The 45° TFBGs were directly inscribed into the core of passive and active (Ho^{3+}:Pr^{3+} co-doped) ZBLAN fibers using an 800 nm wavelength fs laser (1 kHz repetition rate, 115 fs pulse width). During inscription, the fiber was mounted onto a programmable air-bearing translation stage to drive the fiber in a 45° tilted rectangular pattern transversely through the focus of the fs laser. The FBG was written at a translation speed of 80 μm/s corresponding to a spatial overlap between consecutive pulses of approximately 92%. Figure 2(b) shows a differential interference contrast (DIC) microscopic image (top-view) of the femtosecond laser inscribed 45° TFBG within the core of the ZBLAN fiber.

Firstly, we discuss the inscription of 45° TFBGs in passive ZBLAN fiber. Femtosecond laser pulses with an energy of 140 nJ were focused into the core of the fiber using an oil-immersion objective with a numerical aperture (NA) of 0.8. Unlike B/Ge co-doped photosensitive silica fibers, where written index contrasts of $\Delta n \sim 10^{-3}$ have been reported [9], the refractive index modification in ZBLAN fiber is typically on the order of $\sim 10^{-4}$. Consequently, when probed with a supercontinuum broadband source, the polarization dependent loss (PDL) of the TFBG (physical length of 11 mm) was measured to be 3.4 dB. Figure 3 shows the PDL over a large

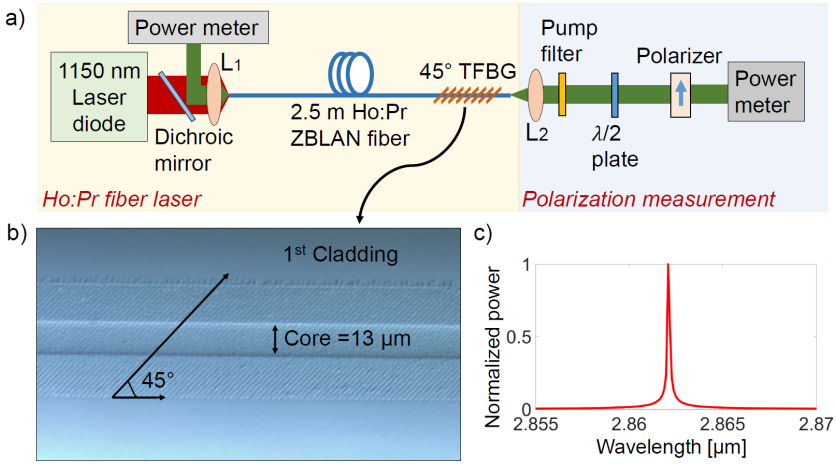

Fig. 2. (a) Experimental setup (b) microscope image of the 45° TFBG in ZBLAN fiber and (c) laser spectrum.

wavelength range of 1.4 μm and the maximum PDL of 3.4 dB was observed at 2.894 μm, the Bragg wavelength of the TFBG as per Eq. (2). The insertion loss of the fabricated in-fiber polarizer was less than 0.5 dB.

The same pulse energy was then used to inscribe gratings into Ho^{3+}:Pr^{3+} co-doped ZBLAN fiber. From this, it was noted that the maximum PDL obtained in the active ZBLAN fiber was only 1.9 dB and therefore much lower than that of the passive fiber. This difference can be explained by the reduced energy that is coupled into the glass matrix and that is therefore eventually available to initiate the refractive index modification. Due to multi-photon absorption by the dopant ions, a part of incident energy is used to excite the active laser ions. This observation is supported by the fluorescence emission that can clearly be seen inside the core when the fs laser beam interacts with the active ZBLAN fiber as shown in Fig. 4. To achieve the same refractive index modification inside the core of the active fiber as in passive fiber, we thus had to increase the pulse energy to 170 nJ. Beyond 170 nJ of pulse energy, damage spots were identified inside the fiber core. Recently, Heck *et al.* also reported a difference in refractive index modification

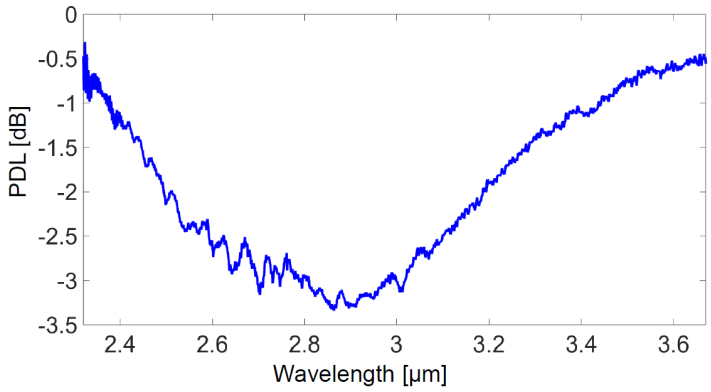

Fig. 3. Polarization dependent loss of 45° TFBG in passive ZBLAN fiber as a function of wavelength.

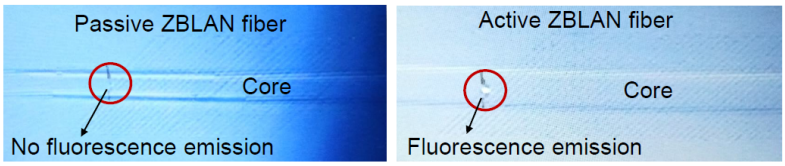

Fig. 4. Direct fs laser inscription of 45° TFBG in passive and active ZBLAN fiber (see Visualization 1).

inside passive and active fluoride fibers [19]. However, further studies are required to completely explain these observations.

4. Polarization measurements of the mid-IR laser with intracavity 45° TFBG

In order to evaluate the PER of the mid-IR fiber laser with intracavity 45° TFBG, we realized a standard Fabry-Perot laser cavity as depicted in Fig. 2(a). The cavity consisted of a perpendicularly cleaved 2.5 m long section of double-clad Ho^{3+}:Pr^{3+} co-doped ZBLAN fiber (molar concentration of 35000: 2500 ppm). The 4% Fresnel reflection from both the ends of the fiber acted as low reflectivity broadband mirrors to form the Fabry-Perot laser cavity. 1.8 W pump power from a multi-mode 1150 nm laser diode was focused into the input end of the active fiber using a CaF_2 lens with a focal length of 20 mm. A free-running lasing peak was observed at 2.862 μm [see Fig. 2(c)] from the laser cavity as the 45° TFBG does not provide wavelength selective feedback to the laser cavity unlike a uniform FBG.

As outlined above, when characterized as an independent polarization device, the PDL of the 45° TFBG was relatively weak (3.4 dB). However, this was sufficient in a resonant cavity to

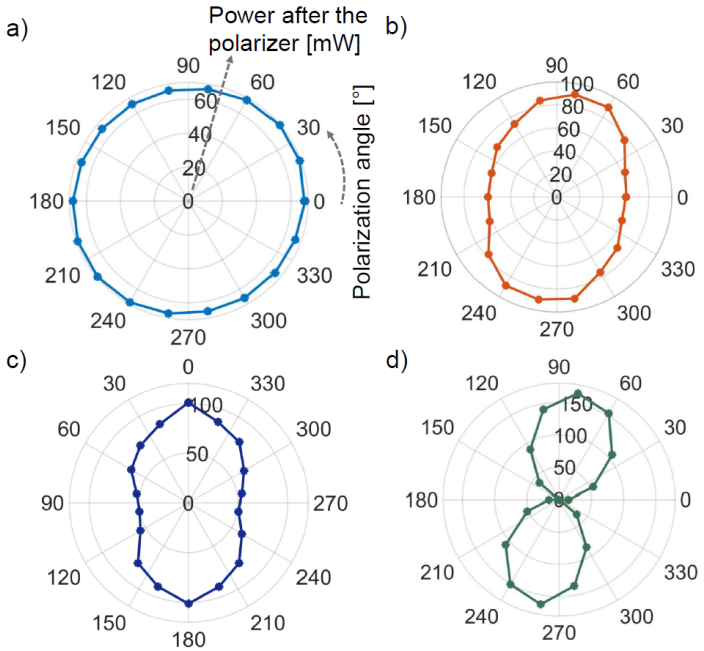

Fig. 5. PER response of the laser (a) without TFBG, (b) with TFBG of 1 mm length, (c) with TFBG of 2 mm length, and (d) with TFBG of 16 mm length.

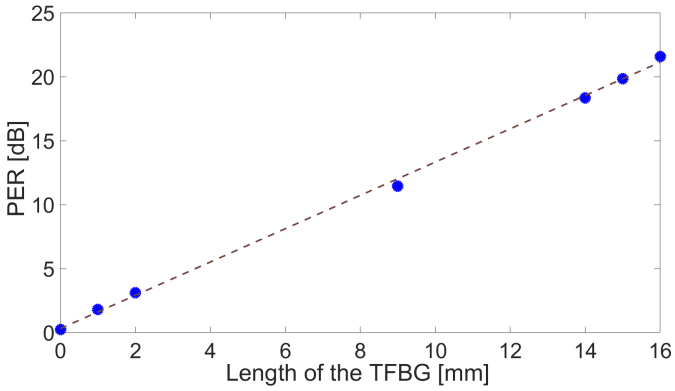

Fig. 6. PER response of the laser as a function of grating length.

achieve a highly linear polarization state with a PER of 21.6 dB. This high PER can be understood by the fact that the TFBG induces higher losses for the *s*-polarized light than *p*-polarized light in each round trip and as a result of gain competition highly linearly polarized laser output is eventually obtained.

To demonstrate the performance of the TFBG, we compare lasers with and without a TFBG in the cavity. In both cases, the experimental setup consisted of a continuous wave (CW) mid-IR laser cavity followed by a dichroic mirror, a collimating lens, a filter to remove any residual pump light, a half-wave plate, a bulk polarizer and a power meter as illustrated in Fig. 2(a). The half-wave plate was used to rotate the polarization of the light emitted from the laser cavity from 0° to 360° which in combination with a free-space polarizer, facilitated the polarization measurement of the fiber laser.

Figures 5(a)–5(d) show the PER response of the CW laser with and without 45° TFBGs of various physical lengths. Figure 5(a) indicates that the CW laser output from the Fabry-Perot laser cavity is unpolarized without the 45° TFBG. Figures 5(b) and 5(c) show the PER response of the laser with 1 mm and 2 mm long 45°TFBGs, respectively. From Fig. 5(d), we can observe that for a 16 mm long TFBG the maximum laser output is achieved at angles around 80° and 260°, while it becomes virtually zero at the orthogonal positions 10° and 170°. The laser output

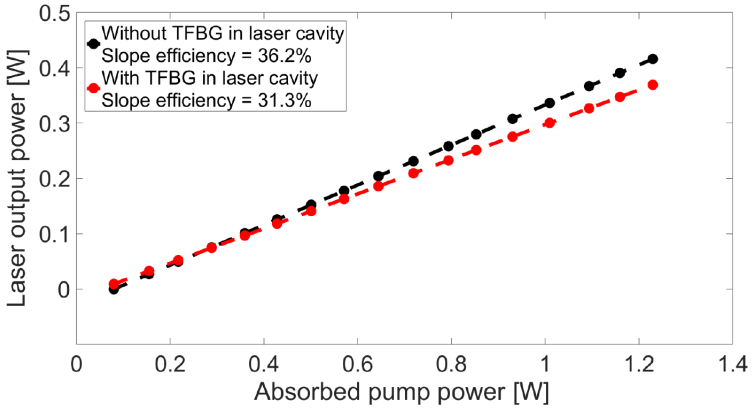

Fig. 7. Slope efficiency of the fiber laser with and without TFBG.

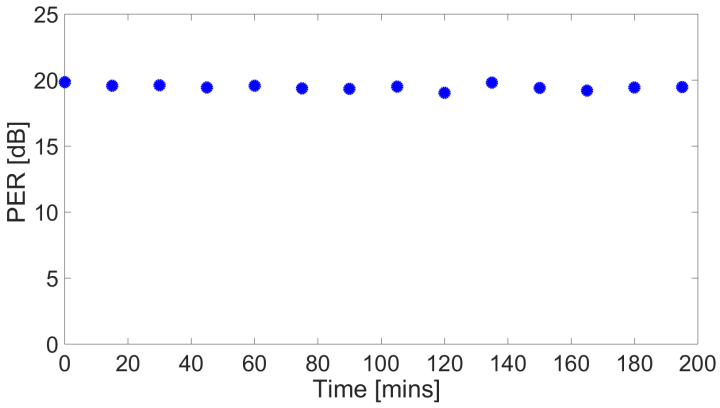

Fig. 8. PER stability of the laser over 3 hours using 15 mm TFBG.

with the TFBG of physical length 16 mm thus shows a maximum PER of 21.6 dB. We also note that as the grating length increases, the polarization response varies from an open figure-8 shape to a fully closed figure-8 shape. Thus, the TFBG with 16 mm physical length acts as a near ideal in-fiber polarizer. It can be also observed that the laser output power after the external polarizer was higher with longer TFBG, as more power is contained in a single polarization axis. Figure 6 shows the PER of the mid-IR fiber laser as a function of grating length. It is noticeable that the extinction ratio increases linearly with the grating length. As the length increases, the higher losses experienced by the *s*-polarized light, result in the observed increase in PER.

The slope efficiency of the mid-IR fiber laser was measured before and after the inscription of a TFBG into the laser cavity. From Fig. 7 it can be observed that, after incorporating the TFBG into the fiber laser cavity the slope efficiency was reduced by ~5%. This variation is most likely due to 45° TFBG induced scattering losses from the fs laser written structures in the core of the fiber. Further, we evaluated the PER stability of the Fabry-Perot laser cavity with the intracavity 45° TFBG of 15 mm physical length for more than 3 hours under laboratory conditions. From Fig. 8 we can see that the PER variation was less than 0.8 dB, which is inconsequential for most laser systems, indicating strong long term stability suitable for many practical applications.

5. Conclusion

In conclusion, we have experimentally evaluated the polarization properties of a 45° TFBG in passive and active ZBLAN fibers. Observations reveal that the PDL of the TFBG fabricated in ZBLAN fiber is relatively weak (3.4 dB) when compared to the PDL reported in the TFBG inscribed in B/Ge co-doped silica fibers (33 dB). This reduction is due to the low refractive index modulation in ZBLAN fiber when compared to the silica fiber. However, when a 16 mm long 45° TFBG was integrated into a mid-IR fiber laser cavity, we could achieve a strong laser output PER of 21.6 dB. It was also noted that the PER variation of the mid-IR fiber laser increases linearly with the grating length. To the best of our knowledge, this is the first demonstration of both in-fiber polarizers for the mid-IR region and a linearly polarized all-fiber mid-IR laser system. This demonstration paves way to the development of all-fiber mid-IR pulsed lasers using nonlinear polarization rotation.

Funding

Air Force Office of Scientific Research (AFOSR) (FA2386-16-1-4030); Australian National Fabrication Facility (OptoFab Node, NCRIS).

OSA CONTINUUM

Acknowledgment

The authors would like to thank Dr. Robert Williams, Dr. Martin Ams, and Thorsten A. Goebel for the helpful discussions.

References

1. T. Erdogan and J. Sipe, "Tilted fiber phase gratings," J. Opt. Soc. Am. A **13**, 296–313 (1996).
2. P. S. Westbrook, T. A. Strasser, and T. Erdogan, "In-line polarimeter Using blazed fiber gratings," IEEE Photon. Technol. Lett. **12**, 1352–1354 (2000).
3. K. Zhou, L. Zhang, X. Chen, and I. Bennion, "Optic sensors of high refractive-index responsivity and low thermal cross sensitivity that use fiber Bragg gratings of > 80° tilted structures," Opt. Lett. **31**, 1193–1195 (2006).
4. Z. Zhang, C. Mou, Z. Yan, K. Zhou, L. Zhang, and S. Turitsyn, "Sub-100 fs mode-locked erbium-doped fiber laser using a 45°-tilted fiber grating," Opt. Express **21**, 28297–28303 (2013).
5. D. D. Hudson, "Invited paper: Short pulse generation in mid-IR fiber lasers," Opt. Fiber Technol. **20**, 631–641 (2014).
6. X. Zhu and N. Peyghambarian, "High-power ZBLAN glass fiber lasers: review and prospect," Adv. Optoelectron. **2010**, 501956 (2010).
7. Y. Yu, X. Gai, P. Ma, K. Vu, Z. Yang, R. Wang, D.-Y. Choi, S. Madden, and B. Luther-Davies, "Experimental demonstration of linearly polarized 2–10 μm supercontinuum generation in a chalcogenide rib waveguide," Opt. Lett. **41**, 958–961 (2016).
8. Z. S. Li, M. Rupinski, J. Zetterberg, Z. T. Alwahabi, and M. Aldén, "Detection of methane with mid-infrared polarization spectroscopy, " Appl. Phys. B: Lasers Opt. **79**, 135–138 (2004).
9. C. Mou, K. Zhou, L. Zhang, and I. Bennion, "Characterization of 45°-tilted fiber grating and its polarization function in fiber ring laser," J. Opt. Soc. Am. B **26**, 1905–1911 (2009).
10. D. D. Hudson, R. J. Williams, M. J. Withford and S. D. Jackson, "Single frequency fiber laser operating at 2.9 μm," Opt. Lett. **38**, 2388–2390 (2013).
11. G. Bharathan, R. I. Woodward, M. Ams, D. D. Hudson, S. D. Jackson, and A. Fuerbach, "Direct inscription of Bragg gratings into coated fluoride fibers for widely tunable and robust mid-infrared lasers," Opt. Express **25**, 30013–30019 (2017).
12. F. Maes, V. Fortin, M. Bernier, and R. Vallée, "5.6 W monolithic fiber laser at 3.55 μm," Opt. Lett. **42**, 2054–2057 (2017).
13. K. Zhou, G. Simpson, X. Chen, L. Zhang, and I. Bennion, "High extinction ratio in-fiber polarizers based on 45° tilted fiber Bragg gratings," Opt. Lett. **30**, 1285–1288 (2005).
14. F. Chen, and J. R. V. de Aldana, "Optical waveguides in crystalline dielectric materials produced by femtosecond laser micromachining," Laser Photon. Rev. **8**, 251–275 (2014).
15. S. Antipov, M. Ams, R. J. Williams, E. Magi, M. J. Withford, and A. Fuerbach, "Direct infrared femtosecond laser inscription of chirped fiber Bragg gratings," Opt. Express **24**, 30–40 (2016).
16. A. Ioannou, A. Theodosiou, C. Caucheteur, and K. Kalli, "Direct writing of plane-by-plane tilted fiber Bragg gratings using a femtosecond laser," Opti. Lett. **42**, 5198–5201 (2017).
17. K. Zhou, L. Zhang, X. Chen, and I. Bennion, "Low thermal sensitivity grating devices based on ex-45° tilting structure capable of forward-propagating cladding modes coupling," J. Lightwave Technol. **24**, 5087–5094 (2006).
18. Z. Yan, C. Mou, K. Zhou, X. Chen, and L. Zhang, "UV-inscription, polarization-dependent loss characteristics and applications of 45° tilted fiber gratings," J. Lightwave Technol. **29**, 2715–2724 (2011).
19. M. Heck, S. Nolte, A. Tünnermann, R. Vallée, and M. Bernier, "Femtosecond-written long-period gratings in fluoride fibers," Opt. Lett. **43**, 1994–1997 (2018).